Eur. Phys. J. Appl. Phys. **52**, 31101 (2010)
DOI: 10.1051/epjap/2010161

THE EUROPEAN PHYSICAL JOURNAL APPLIED PHYSICS

Regular Article

Theoretical interpretation of anomalous tritium and neutron productions during Pd/D co-deposition experiments

Y.E. Kim[a]

Department of Physics, Purdue University, Physics Building, West Lafayette, IN 47907, USA

Received: 2 June 2010 / Received in final form: 27 July 2010 / Accepted: 16 August 2010
Published online: 30 November 2010 – © EDP Sciences

Abstract. The recent experimental observations of triple tracks in solid-state nuclear track detectors, CR-39, during Pd/D co-deposition experiments indicate that the triple tracks are due to ∼14 MeV neutrons, which appear to originate from "hot" fusion reaction D(t,n)^{4}He. Nuclear theory interpretation of the origin of ∼14 MeV neutrons is presented in terms of a sub-threshold resonance reaction involving (T + p) resonance state of ^{4}He$^*(J^\pi = 0^+)$ at 20.21 MeV, which produces 1.01 MeV T. An upper limit of the branching ratio, R(n)/R(T), between neutron production rate and tritium production rate is calculated to be $R(\mathrm{n})/R(\mathrm{T}) < 10^{-4}$. Experimental tests of the proposed theoretical interpretation are proposed.

1 Introduction

Recently, a series of experimental results have been reported on observation of triple tracks in solid-state nuclear track detectors, CR-39, during Pd/D co-deposition experiments [1–4]. Most recent results show that triple tracks in CR-39 detectors observed in Pd/D co-deposition experiments are indistinguishable from those generated upon exposure to a DT neutron source [4]. This experimental observation of "nuclear ashes" is important and significant in establishing the fact that these phenomena observed in the Pd/D co-deposition experiments are due to nuclear reactions.

There have been many reports of anomalous tritium and neutron productions in deuterated metal from electrolysis experiments [5–9] and gas/plasma loading experiments [10–16]. The reported branching ratio of R(n)/R(T) ranges from 10^{-7} to 10^{-9} in contrast to the conventional free-space reactions branching ratio of $R(\mathrm{n})/R(\mathrm{T}) \approx 1$.

In this paper, theoretical interpretation of observed triple tracks from the Pd/D co-deposition experiments [1–4] and anomalous tritium and neutron productions [5–16] is presented in terms of nuclear theory.

In Section 2, a brief summary of present status of experimental results is given. Section 3 discusses deuteron mobility and Bose-Einstein condensation of deuterons. Theoretical interpretation of the observed experimental results of tritium production are given in Section 4. Theoretical interpretation of neutron production is described in Section 5. Experimental tests of theoretical predictions are proposed and described in Section 6. Summary and conclusions are given in Section 7.

[a] e-mail: yekim@purdue.edu

2 Present status of anomalous experimental results

The conventional deuterium fusion in free space proceeds via the following nuclear reactions:

{1} D + D → p (3.02 MeV) + T (1.01 MeV);

{2} D + D → n (2.45 MeV) + ^{3}He (0.82 MeV); and

{3} D + D →^{4}He + γ (23.8 MeV).

The cross-sections (or reaction rates) for reactions {1} and {2} have been measured by beam experiments at intermediate energies (≥10 keV). The cross-sections for reaction {1}–{3} are expected to be extremely small at low energies (≤10 eV) due to the Gamow factor arising from Coulomb barrier between two deuterons. The measured cross-sections have branching ratios: (σ{1}, σ{2}, σ{3}) ≈ (0.5, 0.5, 10^{-6}).

Experimental values of the conventional hot-fusion cross section $\sigma(E)$ for reaction {1} or {2} have been conventionally parameterized as [17]:

$$\sigma(E) = \frac{S(E)}{E}\exp(-2\pi\eta) = \frac{S(E)}{E}\exp\left[-(E_G/E)^{1/2}\right] \quad (1)$$

with $\eta = Z_1Z_2e^2/\hbar\nu$. Exp $(-2\pi\eta)$ is known as the "Gamow factor", and E_G is the "Gamow energy" given by $E_G = (2\pi\alpha Z_D Z_D)^2 Mc^2/2$ or $E_G^{1/2} \approx 31.39$ (keV)$^{1/2}$ for the reduced mass $M \approx M_D/2$ for reactions {1} or {2}. The value E is measured in keV in the center-of-mass (CM) reference frame. The S-factor, $S(E)$, is extracted from experimentally measured values [18] of the cross section $\sigma(E)$ for $E \geq 4$ keV and is nearly constant [19]; $S(E) \approx 52.9$ keV-barn, for reactions {1} or {2} in the energy range of interest here, $E \leq 100$ keV. The S-factor is known as "astrophysical S-factor" [17].

From many experimental measurements by Fleischmann and Pons [20], and many others [5–16,20–23] over 20 years since then, the following experimental results have emerged. At ambient temperatures or low energies (≤10 eV), deuterium fusion in metal proceeds via the following reactions:

{4} D(m) + D(m) → p(m) + T(m) + 4.03 MeV (m);

{5} D(m) + D(m) → n(m) + ^{3}He(m) + 3.27 MeV (m); and

{6} D(m) + D(m) → ^{4}He(m) + 23.8 MeV (m),

where m represents a host metal lattice or metal particle. Reaction rate R for {6} is dominant over reaction rates for {4} and {5}, i.e., $R\{6\} \gg R\{4\}$ and $R\{6\} \gg R\{5\}$.

Experimental observations reported from electrolysis and gas-loading experiments are summarized below (not complete):

(1) The Coulomb barrier between two deuterons are suppressed.
(2) Excess heat production (the amount of excess heat indicates its nuclear origin).
(3) ^{4}He production commensurate with excess heat production, no 23.8 MeV γ-ray.
(4) More tritium is produced than neutron $R\{4\} \gg R\{5\}$.
(5) Production of nuclear ashes with anomalous rates: $R\{4\} \ll R\ \{6\}$ and $R\ \{5\} \ll R\{6\}$.
(6) Production of hot spots and micro-scale craters on metal surface.
(7) Detection of radiations.
(8) "Heat-after-death".
(9) Requirement of deuteron mobility (D/Pd > ∼0.9, electric current, pressure gradient, etc.).
(10) Requirement of deuterium purity (H/D ≪ 1).

All of the above experimental observations are explained either quantitatively or qualitatively in terms of theory of Bose-Einstein condensation nuclear fusion (BECNF) in previous publications [24,25]. In this paper, additional theoretical interpretation is described more in details for observation (4), which involve anomalous production of tritium and neutrons.

3 Deuteron mobility and Bose-Einstein condensation of deuterons in metals

Development of Bose-Einstein condensate theory of deuteron fusion in metal is based upon a single hypothesis that deuterons in metal are mobile and hence are capable of forming Bose-Einstein condensates.

3.1 Deuteron mobility and high-density deuteron-electron plasma in metal

Experimental proof of proton (deuteron) mobility in metals was first demonstrated by Coehn in his hydrogen electromigration experiment [26,27]. A theoretical explanation of Coehn's results [26] is given by Isenberg [28]. The Coehn's experimental fact is not well known in review articles and textbooks.

There are other experimental evidences [29–33] that heating and/or applying an electric field in a metal causes hydrogens and deuterons in a metal to become mobile, thus leading to a higher density for quasi-free mobile deuterons in a metal. It is expected that the number of mobile deuterons will increase, as the loading ratio D/metal of deuterium atoms increases and becomes larger than one, D/metal ≥ 1.

Mobility of deuterons in a metal is a complex phenomenon and may involve a number of different processes [33]: coherent tunneling, incoherent hopping, phonon-assisted processes, thermally activated tunneling, and over-barrier jump/fluid like motion at higher temperatures**.** Furthermore, applied electric fields as in electrolysis experiments can enhance the mobility of absorbed deuterons.

The physical significance of Coehn's results [26] is that a deuterium atom is ionized to become deuteron and an electron, thus creating a high-density deuteron-electron plasma in metal. For the case of PdD, deuteron-electron plasma density of $\sim 10^{22}$ cm^{-3} is achieved in metal.

3.2 BEC fraction of deuterons in metal

Fraction of deuterons in a metal satisfying BEC condition can be estimated as a function of the temperature. The BEC condensate fraction $F(T) = N_{BE}/N$ can be calculated from integrals:

$$N_{BE} = \int_0^{E_C} n(E)N(E)dE \ \text{ and } \ N = \int_0^{\infty} n(E)N(E)dE$$

where $n(E)$ is either Bose-Einstein or Maxwell-Boltzmann distribution function, $N(E)$ is the density of (quantum) states, and E_C is the critical kinetic energy of deuteron satisfying the BEC condition $\lambda_c = d$, where λ_c is the de Broglie wavelength of deuteron corresponding to E_C and d is the average distance between two deuterons. For $d =$ 2.5 Å, we obtain $F\,(T = 300\ \text{K}) \approx 0.084$ (8.4%), $F\,(T = 77.3\ \text{K}) \approx 0.44$ (44%), and $F\,(T = 20.3\ \text{K}) \approx 0.94$ (94%). At $T = 300$ K, $F = 0.084$ (8.4%) is not large enough to form BEC since motions of deuterons are limited to several lattice sites and the probability of their encounters are very small. On the other hand, at liquid nitrogen (77.3 K) and liquid hydrogen (20.3 K) temperatures, probability of forming BEC of deuterons is expected to be $\Omega \approx 1$. This suggests that experiments at these low temperatures can provide tests for enhancement of the reaction rate R_t, equation (4) below, as predicted by BECNF theory.

4 Nuclear theory and theoretical interpretation of experimental data

4.1 Bose-Einstein condensation theory of deuteron fusion in metal

In developing the BEC theory of deuteron fusion in metal, we make one basic assumption that mobile deuterons in

a micro/nano-scale metal particle form a BEC state. The validity of this assumption is to be verified by independent experimental tests suggested in this paper. Because of the above assumption, the theory cannot be applied to deuterons in bulk metals, which do not provide well-defined localized trapping potentials for deuterons.

For applying the concept of the BEC mechanism to deuteron fusion in a nano-scale metal particle, we consider N identical charged Bose nuclei (deuterons) confined in an ion trap (or a metal grain or particle). Some fraction of trapped deuterons are assumed to be mobile as discussed above. The trapping potential is 3-dimensional (nearly-sphere) for nano-scale metal particle, or quasi 2-dimensional (nearly hemi-sphere) for micro-scale metal grains, both having surrounding boundary barriers. The barrier heights or potential depths are expected to be an order of energy ($\leq$1 eV) required for removing a deuteron from a metal grain or particle. For simplicity, we assume an isotropic harmonic potential for the ion trap to obtain order of magnitude estimates of fusion reaction rates.

N-body Schroedinger equation for the system is given by:

$$H\Psi = E\Psi \tag{2}$$

with the Hamiltonian H for the system given by:

$$H = \frac{\hbar^2}{2m}\sum_{i=1}^{N}\Delta_i + \frac{1}{2}m\omega^2\sum_{i=1}^{N}r_i^2 + \sum_{i<j}\frac{e^2}{|r_i - r_j|} \tag{3}$$

where m is the rest mass of the nucleus. Only two-body interactions (Coulomb and nuclear forces) are considered since we expect that three-body interactions are expected to be much weaker than the two-body interactions.

Electron degrees of freedom are not explicitly included, assuming that electrons and host metal atoms provide a host trapping potential. In presence of electrons, the coulomb interaction between two deuterons can be replaced by a screened coulomb potential in equation (3). Hence, equation (3) without the electron screening effect represents the strongest case of the reaction rate suppression due to the coulomb repulsion.

The approximate ground-state solution of equation (2) with H given by equation (3) is obtained using the equivalent linear two-body method [34,35]. The use of an alternative method based on the mean-field theory for bosons yields the same result (see Appendix in [36]). Based on the optical theorem formulation of low energy nuclear reactions [37], the ground-state solution is used to derive the approximate theoretical formula for the deuteron-deuteron fusion rate in an ion trap (micro/nano-scale metal grain or particle). The detailed derivations are given elsewhere including a short-range nuclear strong interaction used [36,38].

Our final theoretical formula for the nuclear fusion rate $R_{\rm trap}$ for a single trap containing N deuterons is given by [24]:

$$R_{\rm trap} = 4\,(3/4\pi)^{3/2}\,\Omega SB\frac{N^2}{D_{\rm trap}^3} \propto \Omega\frac{N^2}{D_{\rm trap}^3} \tag{4}$$

where N is the average number of Bose nuclei in a trap/cluster, $D_{\rm trap}$ is the average diameter of the trap, $B = 2r_B/(\pi\hbar)$, $r_B = \hbar^2/(2\mu e^2)$, and S is the S-factor for the nuclear fusion reaction between two deuterons, as defined by equation (1). For D(d,p)T and D(d,n)^{3}He reactions, we have $S \approx 55$ keV-barn. We expect also $S \approx 55$ keV-barn or larger for reaction {6}. $B = 1.4 \times 10^{-18}$ cm^3/s with S in units of keV-barn in equation (4). $SB = 0.77 \times 10^{-16}$ cm^3/s for $S = 55$ keV-barn. Unknown parameters are the probability of the BEC ground state occupation, Ω and the S-factor, S, for each exit reaction channel. We note that $\Omega \leq 1$.

The total fusion rate R_t is given by:

$$R_t = N_{\rm trap}R_{\rm trap} = \frac{N_D}{N}R_{\rm trap} \propto \Omega\frac{N}{D_{\rm trap}^3} \tag{5}$$

where N_D is the total number of deuterons and $N_{\rm trap} = N_D/N$ is the total number of traps.

Equation (5) shows that the total fusion rates, R_t, are very large if $\Omega \approx 1$.

The total reaction rate R_t for each exit reaction channel can be calculated for given values of Ω and S, using equations (4) and (5). The S-factor can be either inferred from experimental data or can be calculated theoretically using equation (9) (see Sect. 4.3 and Appendix). The branching ratio between two different exit reaction channels can be obtained as the ratio between two S-factors (see Tab. 2 in Sect. 5.1).

Equations (4) and (5) provide an important result that nuclear fusion rates $R_{\rm trap}$ and R_t do not depend on the Gamow factor in contrast to the conventional theory for nuclear fusion in free space. This could provide explanations for overcoming the Coulomb barrier and for the claimed anomalous effects for low-energy nuclear reactions in metals. This is consistent with the conjecture noted by Dirac [39] and used by Bogoliubov [40] that boson creation and annihilation operators can be treated simply as numbers when the ground state occupation number is large. This implies that for large N each charged boson behaves as an independent particle in a common average background potential and the Coulomb interaction between two charged bosons is suppressed. This provides an explanation for the observation (1). There is a simple classical analogy of the Coulomb field suppression. For an uniform charge distribution in a sphere, the electric field is a maximum at the surface of the sphere and decreases to zero at the center of the sphere.

4.2 Sub-threshold resonance reactions

In this section, we present a theoretical explanation of this anomalous tritium production based on the BECNF theory, utilizing a sub-threshold resonance ^{4}He* (0^+) state at 20.21 MeV with a resonance width of Γ(T + p) = 0.5 MeV as shown in Figure 1.

In Figure 1, reaction channels {4}, {5}, and {6} described in Section 2 are shown. Entrance channel {7}, and exit channels {7a} and {7b} (described below) are also

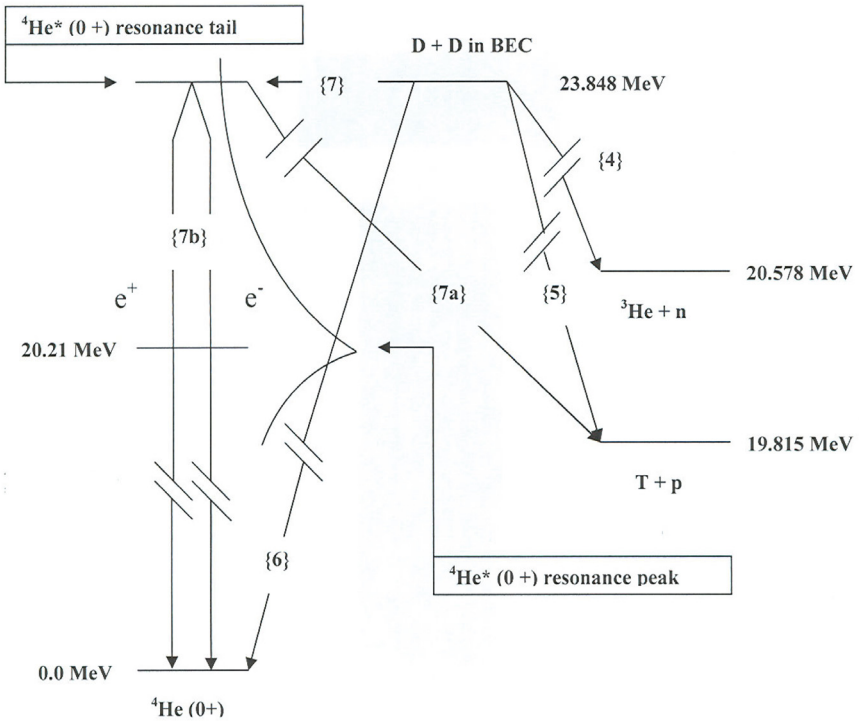

Fig. 1. Exit reaction channels for D + D fusion in Bose-Einstein condensate state. Parallel bars indicate break in energy scale.

shown. Due to a selection rule derived in reference [24], both {4} and {5} are suppressed, and we have $R\{4\} \ll R\{6\}$ and $R\{5\} \ll R\{6\}$. In free space, {6} would be forbidden due to the momentum conservation, while {7} would satisfy the momentum conservation for $Q = 0$. For this section (Eqs. (8)–(11)), we use a new energy level scale which sets $E = 0$ for (D + D) state, and $E = -23.85$ MeV for the ^{4}He ground state. Q-value remains same since $Q = E_i - E_f$.

Above the ground-state of ^{4}He, there are five excited continuum states, ^{4}He* (J^π, T), below the (D + D) threshold energy [41]: (0^+, 0, 20.21 MeV), (0^-, 0, 21.01 MeV), (2^-, 0, 21.84 MeV), (2^-, 1, 23.33 MeV), and (1^-, 1, 23.64 MeV). In this paper, we consider reaction rates for two exit channels to ^{4}He (0^+, 0, 0.0 MeV) and ^{4}He* (0^+, 0, 20.21 MeV) states.

For a single trap (or metal particle) containing N deuterons, the deuteron-deuteron fusion can proceed with the following two reaction channels:

$$\{6\}\ \psi_{\rm BEC}\left\{(N-2)\,{\rm D's} + ({\rm D}+{\rm D})\right\} \rightarrow \psi^*\left\{^4{\rm He}\,(0^+,0) + (N-2)\,{\rm D's}\right\} \quad (6)$$

and

$$\{7\}\ \psi_{\rm BEC}\left\{(N-2)\,{\rm D's} + ({\rm D}+{\rm D})\right\} \rightarrow \psi^*\left\{^4{\rm He}^*\,(0^+,0) + (N-2)\,{\rm D's}\right\} \quad (7)$$

where $\psi_{\rm BEC}$ is the Bose-Einstein condensate ground state (a coherent quantum state) with N deuterons and ψ^* are final excited continuum states. ^{4}He in equation (6) represents the ground state with spin-parity, 0^+, while ^{4}He* in equation (7) represents the 0^+ excited state at 20.21 MeV with the resonance width of Γ(T + p) = 0.5 MeV above the ^{4}He ground state [41]. It is assumed that excess energy (Q value) is absorbed by the BEC state and shared by $(N - 2)$ deuterons and reaction products in the final state. It is important to note that reaction {6}, described by equation (6), cannot occur in free space due to the momentum conservation, while reaction {7} described by equation (7) can occur with $Q = 0$ in free space without violating the momentum conservation, due to the resonance width of Γ(T+p) = 0.5 MeV [41] for the 20.21 MeV state of ^{4}He*. A detailed description of reaction {6} is given in previous publications [24,25]. In the following, detailed description and discussion of reaction {7} are given.

The reaction {7}, described by equation (7), can proceed via a sub-threshold resonance reaction [42–47]. The cross section for the sub-threshold resonance reaction is given by Breit-Wigner expression:

$$\sigma(E) = \pi\lambda\!\!\!^{-2} w \frac{\Gamma_i(E)\Gamma_f}{(E-E_R)^2 + (\Gamma/2)^2} \quad (8)$$

where $\lambda\!\!\!^{-} = \lambda/2\pi$, $\lambda = h/mv$ (de Broglie wavelength), w is a statistical factor, E_R is the sub-threshold resonance energy. Γ_f is a partial decay width and Γ is the total decay width to the final states. If E is measured from the threshold energy $E = 0$ of (D + D) state, E_R = (20.21 MeV – 23.85 MeV) = – 3.64 MeV.

4.3 Determination of S-factor and reaction rates

After combining equation (1) with equation (8), the $S(E)$ factor can be written as [42,47]:

$$S(E) = E \exp(2\pi\eta)\, \pi\lambda\!\!\!^{-2} w \frac{\Gamma_i(E)\Gamma_f}{(E-E_R)^2 + (\Gamma/2)^2}. \quad (9)$$

The $S(E)$ factor near zero energy for the $\ell = 0$ state can then be written as (see Appendix for detailed derivation):

$$S(E) = \frac{\pi^2\hbar^4}{4\mu^2 R_n^2} \frac{1}{K_1^2(x)} w\theta_0^2 F_{\rm BW}(E), \quad (10)$$

with

$$F_{\rm BW}(E) = \frac{\Gamma_f}{(E-E_R)^2 + (\Gamma/2)^2} \quad (11)$$

where μ is the reduced mass in units of atomic mass unit (931.494 MeV), R_n is the nuclear radius, and $K_1(x)$ is the modified Bessel function of order unity with argument $x = (8Z_1Z_2e^2R_n\mu/\hbar^2)^{1/2}$. $K_1(x)$ is related to irregular Coulomb wave function $G_0(E, R_n)$ [48,49] (see Appendix). We note that $F_{\rm BW}(E_R)$ is a maximum at $E = E_R = -3.64$ MeV. At $E = 0$, $F_{\rm BW}(0)$ is reduced to $F_{\rm BW}(0) = 0.47 \times 10^{-2} F_{\rm BW}(E_R)$. Equation (10) shows that the $S(E)$ factor has a finite value at $E = 0$ and drops off rapidly with increasing energy E. θ_i^2 is the reduced width of a nuclear state [44], representing the probability of finding the excited state in the configuration i, and the sum of θ_i^2 over i is normalized to 1. θ_i is the overlap integral between the initial and final nuclear state components, $\langle\psi_{\rm final}|\psi_{\rm initial}\rangle$. The dimensionless number θ_i^2 is generally determined experimentally and contains the nuclear structure information.

Equations (10) and (11) were used extensively in analysis of (p,γ) reactions involved in nucleosynthesis processes in astrophysics [17,43,45–47].

Once $S(E)$ is calculated using equations (10) and (11), the reaction rates can be calculated from equations (4) and (5), using the calculated values of $S(E)$.

4.4 Reaction rates for anomalous production of tritium

For the entrance channel {7}, D + D $\rightarrow{}^4$He* (0^+, 0, 23.85 MeV, $Q = 0$), there are two possible decay channels as shown in Figure 1:

{7a} ^{4}He* (0^+, 0) $\rightarrow$ T (1.01 MeV) + p (3.02 MeV)

{7b} ^{4}He* (0^+, 0) $\rightarrow{}^4$ He ($0^+, 0, 0.0$ MeV) (ground state).

$S(E)$ factors are calculated from equation (10) using $E = 0$ at a tail of the ^{4}He* (0^+, 0) resonance at 20.21 MeV. $E = 0$ corresponds to 23.85 MeV above ^{4}He (0^+, 0) ground state. The calculated $S(E)$ can be used in equations (3) and (4) to obtain the total fusion reaction rate. We will estimate $S(E)$ factors for the decay channels, {7a} and {7b}, using equation (10) in the following.

For the decay channel {7a}, $\Gamma_f = \Gamma\{7a\} = 0.5$ MeV [41]. When this value of Γ_f is combined with other appropriate inputs in equation (10), the extracted S-factor for the decay channel {7a} is $S\{7a\} \approx 1.4 \times 10^2$ $[\theta\{7\}]^2$ keV-barn for $E \approx 0$. In reference [24], it was shown that the neutron production rate $R\{5\}$ is suppressed, i.e. $R\{5\} \ll R\{6\}$ due to a selection rule. Since (^{3}He + n) state has a resonance width of $\Gamma_f(^3\text{He} + \text{n}) = 0$ [41], this value of $S\{7a\}$ may provide an explanation of the reported branching ratio of $R(\text{T})/R(\text{n}) \approx 10^7$–$10^9$ [10–16] or $R(\text{n})/R(\text{T}) \approx 10^{-7}$–$10^{-9}$, as shown below.

For the decay channel {7b} ($0^+ \rightarrow 0^+$ transition), γ-ray transition is forbidden. However, the transition can proceed via the internal e^+e^- pair conversion. The transition rate for the internal electron pair conversion is given by:

$$\omega = \frac{1}{135\pi}\left(\frac{e^2}{\hbar c}\right)^2 \frac{\gamma^5}{\hbar^5 c^4} R_N^4,$$
$$R_N^2 = \left|\left\langle \psi_{\rm exc}, \sum_i r_i^2 \psi_{\rm g.s.}\right\rangle\right| \approx R_n^2\phi \quad (12)$$

where γ is the transition energy, R_n is the nuclear radius, and $\phi = \langle\psi_{\rm exc}|\psi_{\rm g.s.}\rangle$, which is the overlap integral between the initial and final nuclear state components. Equation (12) was derived by Oppenheimer and Schwinger [50] in 1939 for their theoretical investigation of $0^+ \rightarrow 0^+$ transition in ^{16}O. The rate for the internal electron conversion is much smaller by many order of magnitude.

For our case of $0^+ \rightarrow 0^+$ transition {7b}, we obtain $\omega \approx 1.75 \times 10^{13}\,\text{s}^{-1}$, and $\Gamma_f = \hbar\omega \approx 1.15 \times 10^{-2}$ eV using appropriate inputs in equation (12). Using $\Gamma_f = \Gamma\{7b\} = 1.15 \times 10^{-2}$ eV in equation (11), the extracted S-factor for decay channel {7b} is $S\{7b\} \approx 3.3 \times 10^{-6}$ $[\theta\{7\}]^2$ $[\phi\{7b\}]^2$ keV-barn for $E \approx 0$, yielding a branching ratio, $R\{7b\}/R\{7a\} \approx S\{7b\}/S\{7a\} \approx 2.4 \times 10^{-8}[\phi\{7b\}]^2$. Experiments are needed for testing this predicted branching ratio.

5 Theoretical interpretation of reaction rates for neutron production

Experimental observation of $R(\text{n})/R(\text{T}) \approx 10^{-7}$–$10^{-9}$ [10–16] is anomalous since we expect $R(\text{n})/R(\text{T}) \approx 1$ from "hot" fusion reactions, {1} and {2}. In this section, we explore nuclear reactions producing neutrons at anomalously low rates.

There are four possible processes which can produce neutrons. The first process is the secondary "hot" fusion reaction {2} producing 2.45 MeV neutrons. The rate for this secondary reaction is extremely small, $R\{2\}/R\{6\} = R(\text{n})/R(^4\text{He}) < 10^{-11}$, as shown previously [25].

The second process is 3D BECNF reaction. In reference [24], it is shown that both reaction {4} and {5} are suppressed due to a selection rule [24]. It was also suggested that the following 3D BECNF is possible:

{8} D + D + D (in BEC state) $\rightarrow$ n + p + ^{4}He + 21.6 MeV.

This reaction is a secondary effect since the probability for {8} is expected to be much smaller than 2D BECNF

reaction {6}. Furthermore, it is suppressed further due to the selection rule described in [24].

The third process is a "hot" fusion reaction D(t, n)^{4}He:

$$\{9a\}\ \ \mathrm{T} + \mathrm{D} \rightarrow \mathrm{n} + {}^4\mathrm{He},\ Q = 17.59\ \mathrm{MeV}$$

induced by 1.01 MeV T produced from reaction {7a}. Since the cross-section for reaction {9a} is large and a maximum (several barns) at $E_D \approx 100$ keV [51], neutrons from this process may contribute substantially to the branching ratio $R(\mathrm{n})/R(\mathrm{T}) = 10^{-7}$–$10^{-9}$, as discussed in the next section.

Since Mosier-Boss et al. [4] used 0.03 M $PdCl_2$ and 0.3 M LiCl in D_2O in their experiment [4], there is a possibility that a fourth process {9b}, ^{7}Li(t, n)^{9}Be, may be involved in generating energetic neutrons:

$$\{9b\}\ \ \mathrm{T} + {}^7\mathrm{Li} \rightarrow \mathrm{n} + {}^9\mathrm{Be},\ Q = 10.439\ \mathrm{MeV}.$$

The neutron production rate for {9b} is expected to be much smaller than that for {9a}. Energetic neutrons from the third process {9a} and the fourth process {9b} described above could induce the following reactions:

$$\{10\}\ {}^{12}\mathrm{C}\,(\mathrm{n},\mathrm{n}')\,3\,{}^4\mathrm{He},\ {}^{12}\mathrm{C}\,(\mathrm{n},\mathrm{n}'\alpha)\,{}^8\mathrm{Be}\,({}^8\mathrm{Be}\rightarrow 2\,{}^4\mathrm{He}),\ \text{etc.}$$

as reported recently by Mosier-Boss et al. [1–4].

5.1 Branching ratios between neutron and tritium productions

The probability $P(E_i)$ for a triton to undergo the conventional hot-fusion reaction {9a} while slowing down in the deuterated palladium metal can be written as [52]:

$$P(E_i) = 1 - \exp\left[\int dx n_D \sigma\left(E_{TD}\right)\right] \approx \int dx n_D \sigma\left(E_{TD}\right) = n_D \int_0^{E_i} dE_T \frac{1}{|dE_T/dx|}\sigma\left(E_{TD}\right). \quad (13)$$

Quantities E_T and E_{TD} are the triton kinetic energies in the LAB and CM frames respectively. The stopping power for triton in PdD for $E_T \leq 3$ MeV can be obtained from the following formula [53].

The stopping power for a proton by the target atom j with the density n_j^t is taken from reference [53]. For a proton laboratory kinetic energy of $E \leq 10$ keV, it is given by:

$$\frac{dE}{dx} = n_j^t A_1 E^{1/2} \times 10^{-18}\ \mathrm{keV\,cm^2}. \quad (14)$$

For 10 keV $\leq E \leq 1$ MeV, it is given by

$$\left[\frac{dE}{dx}\right]^{-1} = \left[\frac{dE}{dx}\right]_{\mathrm{slow}}^{-1} + \left[\frac{dE}{dx}\right]_{\mathrm{high}}^{-1}, \quad (15)$$

where

$$\left[\frac{dE}{dx}\right]_{\mathrm{slow}} = n_j^t A_2 E^{0.45} \times 10^{-18}\ \mathrm{keV\,cm^2}, \quad (16)$$

Table 1. Stopping power coefficients [53].

Element (z)	H (1)	O (8)	Ti (22)	Pd (46)
A_1	1.262	2.652	4.862	5.238
A_2	1.44	3	5.496	5.9
A_3	242.6	1920	5165	1.038×10^4
A_4	1.2×10^4	2000	568.5	630
A_5	0.1159	0.0223	0.009474	0.004758

and

$$\left[\frac{dE}{dx}\right]_{\mathrm{high}} = n_j^t (A_3/E) \ln\left[(A_4/E) + (A_5 E)\right] \times 10^{-18}\ \mathrm{keV\,cm^2}. \quad (17)$$

The coefficients A_1 through A_5 are given in Table 1 above [53].

For the case of triton with laboratory kinetic energy of $E \leq 3$ MeV, E in equations (14)–(17) is to be replaced by $E/3$.

For the case of PdD, the target densities are assumed to be $n_{\mathrm{Pd}}^t = n_{\mathrm{D}} = 6.8 \times 10^{22}$ cm^{-3}. For the incident triton with a kinetic energy (lab) of $E_i = 1.01$ MeV, equation (13) yields $P(E_i) = 0.31 \times 10^{-4}$, and hence the branching ratio of $R(\mathrm{n})/R(\mathrm{T}) = 0.31 \times 10^{-4}$ in PdD.

For the case of D_2O, with $n_{\mathrm{O}}^t = 3.3 \times 10^{22}$ cm^{-3} and $n_{\mathrm{D}}^t = n_{\mathrm{D}} = 6.6 \times 10^{22}$ cm^{-3}, we obtain the calculated value of $P(E_i) = 0.94 \times 10^{-4}$ and the branching ratio $R(\mathrm{n})/R(\mathrm{T}) = 0.94 \times 10^{-4}$ in the heavy water.

For the case of TiD, with $n_{\mathrm{Ti}}^t = n_{\mathrm{D}} = 5.68 \times 10^{22}$ cm^{-3}, we obtain the calculated value of $P(E_i) = 0.37 \times 10^{-4}$ and the branching ratio $R(\mathrm{n})/R(\mathrm{T}) = 0.37 \times 10^{-4}$.

From the above calculated results with PdD, D_2O, and TiD, we have $R(\mathrm{n})/R(\mathrm{T}) < 10^{-4}$. The calculated results of the S-factors for different exit reaction channels are summarized in Table 2. The calculated branching ratio, $R(\mathrm{n})/R(\mathrm{T})$, is also shown in Table 2.

5.2 Range of tritons

The range $\Delta x(E_i)$ of triton in PdD can be calculated as

$$\Delta x(E_i) = \int dx = \int_0^{E_i} \left(\frac{dE}{dx}\right)^{-1} dE. \quad (18)$$

For the case of PdD with $E_i = 1.01$ MeV, the calculated value of the range using equation (18) is $\Delta x(E_i) = 0.42 \times 10^{-3}$ cm, while $\Delta x(E_i) = 1.4 \times 10^{-3}$ cm for the case of D_2O. For the case of TiD, $\Delta x(E_i) = 0.64 \times 10^{-3}$ cm.

Because of different ranges of 1.01 MeV triton in different surrounding media (PdD, D_2O, and TiD) with different extents of media, the branching ratios of $R(\mathrm{n})/R(\mathrm{T}) = 0.31 \times 10^{-4}$, 0.94×10^{-4}, and 0.37×10^{-4} in PdD, D_2O, and TiD as calculated in Section 5.1 are upper limits since the branching ratio $R(\mathrm{n})/R(\mathrm{T})$ depends on deuteron density and extent of deuterons surrounding 1.01 MeV triton produced from reaction {7a}. Thus reported values of

Table 2. S-factors for Reactions in BECNF $\theta^2(\text{or } \phi^2) = |\langle\psi_f|\psi_i\rangle|^2$.

Reactions	Reaction types/ Products	S-factor (keV-barn)
{7a} ^{4}He* (0^+, STR, 23.85 MeV) $\rightarrow$ T (1.01 MeV) + p (3.02 MeV) $Q = 4.03$ MeV	Sub-threshold Resonance reaction/ Tritium, proton, heat	$\sim 1.4 \times 10^2$ $[\theta\{7\}]^2$
{7b} ^{4}He* (0^+, STR, 23.85 MeV) $\rightarrow$ ^{4}He (0^+, g.s., 0.0 MeV) + e^+e^- pair $Q = 23.85$ MeV	Sub-threshold Resonance reaction/ ^{4}He, e^+e^-, γ, heat	$\sim 3.3 \times 10^{-6}$ $[\theta\{7\}]^2$ $[\phi\{7b\}]^2$
{11} T + D $\rightarrow$ n (14.07 MeV) + ^{4}He (3.51 MeV), $Q = 17.59$ MeV	Direct reaction (Hot fusion)/ Neutron, ^{4}He, heat	$R(\text{n})/R(\text{T}) = S(\text{n})/S(\text{T})$ $S\{11\}/S\{7a\} < 10^{-4}$

$R(\text{n})/R(\text{T}) \approx 10^{-7}$ and 10^{-9} from the gas-loading experiments [10–16] are consistent with the calculated upper limit, $R(\text{n})/R(\text{T}) < 10^{-4}$, as discussed in Section 5.1.

6 Proposed experimental tests of theoretical predictions

To test the above theoretical interpretation, based on the third process {9a}, we need to measure/detect (i) 1.01 MeV tritium production and 3.02 MeV proton production from reaction {9a}, (ii) Bremsstrahlung radiations from energetic electrons going through metal, (iii) 0.51 MeV γ-rays from e^+e^- annihilation, (iv) energetic electrons from e^+e^- pair production, (v) γ-rays from secondary reactions (see below).

For (i) detection of 1.01 MeV tritons, it may be necessary to design new experimental set-ups capable of counting 1.01 MeV tritons directly. Alternative method would be to use Ti/D systems as done in [10].

Tritium with a half life of ~12.3 years emits a low energy β particle (e^-) with an end-point energy of 18.6 KeV and an average energy of 5.7 KeV. The range of β with the maximum energy is as small as 9 mg/cm^2 (in medium Z materials). Tritium located only within this range can be detected by direct counting β particle, which may be very inefficient. However, in the case of titanium samples, the energetic upper half of the β spectrum is able to excite the characteristic Kα (4.5 KeV) and Kβ (4.9 KeV) X-rays of titanium. This does not happen in Pd, since Pd has characteristic K X-rays with energies greater than 21 KeV. Therefore, the use of Ti/D instead of Pd/D is proposed for future experimental tests.

For (iii), it could be accomplished by performing a coincidence measurement on the two 0.51 gamma-rays that are emitted in positron annihilation. The use of two high purity germanium (HPGe) detectors in close to the electrodes might be efficient enough to detect the annihilation gamma-rays.

For (v) detection of γ-rays from secondary reactions, we may consider the following reactions:

$$\{11\}\ \text{n} + \text{D} \rightarrow \text{T} + \gamma + 6.257\ \text{MeV},$$

induced by energetic neutrons from {9a}, and also γ-rays from reaction {12} induced by 3.2 MeV protons from {7a}:

$$\{12\}\ \text{p} + \text{D} \rightarrow^3 \text{He} + \gamma + 5.494\ \text{MeV}.$$

The cross-section for {11} with thermal neutrons is ~0.5 mb.

7 Summary and conclusions

Based on both the recently developed theory of Bose-Einstein condensation mechanism [24,25] for the entrance reaction channel, D + D reaction, in metal and the nuclear theory of the sub-threshold resonance reaction mechanism for the exit reaction channel, the reaction rate for 1.01 MeV T from the exit reaction channel {7a} is calculated. The neutron production rate is also estimated as a secondary reaction, D(t, n)^{4}He, using the conventional nuclear theory. An upper limit of the branching ratio, $R(\text{n})/R(\text{T})$, between the neutron and triton reaction rates is estimated to be $R(\text{n})/R(\text{T}) < 10^{-4}$. A set of experiments for testing theoretical predictions is proposed, in order to confirm the theoretical predictions and/or improve theoretical descriptions.

Appendix

In this Appendix, a detailed derivation is given for extraction of S-factor for the sub-threshold resonance reaction. The original derivation and results are given in references [42] and [47]. The cross section for reaction through compound nucleus resonance state is given by:

$$\sigma(E) = \pi\lambda\!\!\!^{-2} w \frac{\Gamma_i(E)\Gamma_f}{(E - E_R)^2 + (\Gamma/2)^2} \qquad \text{(A.1)}$$

where $\lambda\!\!\!^{-} = \frac{1}{2\pi}\lambda$ and λ is de Broglie wave-length, $\lambda = h/mv$, and w is the statistical factor given by:

$$w = \frac{2J+1}{(2J_i+1)(2J_f+1)}(1 + \delta_{if}). \qquad \text{(A.2)}$$

To extract $S(E)$ from (A.1), we use $S(E)$ defined by the following definition of $S(E)$ [17]:

$$\sigma(E) = \frac{S(E)}{E} e^{-2\pi\eta}, \tag{A.3}$$

with $\eta = Z_1 Z_2 e^2/\hbar\nu$.

Equating (A.1) and (A.3), we obtain:

$$S(E) = E e^{2\pi\eta} \pi \lambda\!\!\!^{-2} w \frac{\Gamma_i(E)\Gamma_f}{(E - E_R)^2 + (\Gamma/2)^2} \tag{A.4}$$

with

$$\Gamma_{i,\ell}(E) = \frac{2\hbar}{R_n} \left(\frac{2E}{\mu}\right)^{1/2} P_\ell(E, R_n)\theta_\ell^2 \tag{A.5}$$

where μ is the reduced mass.

The penetration factor $P_\ell(E, R_n)$ in equation (A.5) is given by:

$$P_\ell(E, R_n) = \frac{1}{F_\ell^2(E, R_n) + G_\ell^2(E, R_n)}, \tag{A.6}$$

where R_n is the nuclear radius, and F_ℓ and G_ℓ are regular and irregular Coulomb wave functions [48].

For the s-wave ($\ell = 0$) formation of the compound nucleus at energies E near zero, we have $F_0(E, R_n) \approx 0$ and

$$G_0(E, R_n) \approx 2e^{\pi\eta} \left(\frac{\rho}{\pi}\right)^{1/2} K_1(x), \tag{A.7}$$

where $x = 2\sqrt{2\eta\rho}$, $\rho = \sqrt{2\mu E} R_n/\hbar$, and $K_1(x)$ is the modified Bessel function of order one [49]. The argument x is given by $x = (8Z_1 Z_2 e^2 R_n \mu/\hbar^2)^{1/2} = 0.525(\mu Z_1 Z_2 R_n)^{1/2}$, and μ is the reduced mass in units of atomic mass unit (931.494 MeV).

The penetration factor for $\ell = 0, P_0(E, R_n)$, is then given by:

$$P_0(E, R_n) \approx \frac{1}{G_0^2(E, R_n)} = \frac{\pi}{4\rho K_1^2(x)} e^{-2\pi\eta} \tag{A.8}$$

and the compound nucleus formation width, $\Gamma_{i,0}(E)$, is

$$\Gamma_{i,0}(E) = \frac{\pi\hbar^2}{2\mu R_n^2} \frac{I}{K_1^2(x)} \theta_0^2 e^{-2\pi\eta} \tag{A.9}$$

where θ_ℓ^2 is called the reduced width of a nuclear state, which is generally determined experimentally and contains the nuclear structure information. θ_ℓ^2 is dimensionless and $\theta_\ell^2 \leq 1$ (called Wigner limit) [42]. θ_ℓ^2 is normalized as $\sum \theta_\ell^2 = 1$.

The $S(E)$ factor, equation (A.4), near zero energies can now be written as [47]:

$$S(E) = \frac{\pi^2\hbar^4}{4\mu^2 R_n^2} \frac{1}{K_1^2(x)} w\theta_0^2 F_{\mathrm{BW}}(E) \tag{A.10}$$

where

$$F_{\mathrm{BW}}(E) = \frac{\Gamma_f}{(E - E_R)^2 + (\Gamma/2)^2}. \tag{A.11}$$

References

1. P.A. Mosier-Boss, S. Szpak, F.E. Gordon, L.P.G. Forsley, Eur. Phys. J. Appl. Phys. **40**, 293 (2007)
2. P.A. Mosier-Boss, S. Szpak, F.E. Gordon, L.P.G. Forsley, Naturwissenschaften **96**, 135 (2009)
3. P.A. Mosier-Boss, S. Szpak, F.E. Gordon, L.P.G. Forsley, Eur. Phys. J. Appl. Phys. **46**, 30901 (2009)
4. P.A. Mosier-Boss, J.Y. Dea, L.P.G. Forsley, M.S. Morey, J.R. Tinsley, J.P. Hurley, F.E. Gordon, Eur. Phys. J. Appl. Phys. **51**, 20901 (2010)
5. E. Storm, C. Talcott, Fus. Technol. **17**, 680 (1990)
6. K. Cedzynska, S.C. Barrowes, H.E. Bergeson, L.C. Knight, F.W. Will, Fus. Technol. **20**, 108 (1991)
7. F.G. Will, K. Cedzynska, D.C. Linton, J. Electroanal. Chem. **360**, 161 (1993); F.G. Will, K. Cedzynska, D.C. Linton, Trans. Fus. Technol. **26**, 209 (1994)
8. J.O'M. Bockris, C.-C. Chien, D. Hodko, Z. Minevski, Tritium and Helium Production in Palladium Electrodes and the Fugacity of Deuterium Therein, Frontiers Science Series No. 4, in *Proc. Third Int. Conf. on Cold Fusion, Nagoya, Japan*, edited by H. Ikegami (Universal Academy Press Tokyo, Japan, 1993), p. 23
9. R. Szpak, P.A. Mosier-Boss, R.D. Boss, J.J. Smith, Fus. Technol. **33**, 38 (1998)
10. M. Srinivasan et al., AIP Conf. Proc. **228**, 514 (1990)
11. A. DeNinno, A. Frattolillo, G. Lollobattista, L. Martinis, M. Martone, L. Mori, S. Podda, F. Scaramuzzi, II Nuovo Cimento A **101**, 841 (1989)
12. T.N. Claytor, D.G. Tuggle, H.O. Menlove, P.A. Seeger, W.R. Doty, R.K. Rohwer, Tritium and Neutron Measurements from a Solid-State Cell, Los Alamos National Laboratory report LA-UR-89-3946, October 1989, presented at the NSF-EPRI Workshop
13. T.N. Claytor, D.G. Tuggle, H.O. Menlove, P.A. Seeger, W.R. Doty, R.K. Rohwer, Tritium and Neutron Measurements from Deuterated Pd-Si, AIP Conf. Proc. **228**, *Anomalous Nuclear Effects in Deuterium/Solid Systems*, edited by S. Jones, F. Scaramuzzi, D. Worledge (Provo, Utah, 1990), p. 467
14. T.N. Claytor, D.G. Tuggle, S.F. Taylor, Evolution of Tritium from Deuterided Palladium Subject to High Electrical Currents, Frontiers Science Series No. 4, in *Proc. Third Int. Conf. on Cold Fusion, Nagoya, Japan*, edited by H. Ikegami (Universal Academy Press Tokyo, Japan, 1993), p. 217
15. T.N. Claytor, D.G. Tuggle, S.F. Taylor, Tritium Evolution from Various Morphologies of Deuterided Palladium, in *Proc. Fourth Int. Conf. on Cold Fusion, Maui, Hawaii, 1993*, edited by T.O. Passel, EPRI-TR-104188-V1 Project 3170 (1994), Vol. 1, 7–2
16. T.N. Claytor et al., Tritium Production from Palladium Alloys, in *Proc. ICCF-7, Vancouver, Canada* (ENECO, Inc., Salt Lake City, USA, 1998), p. 88
17. W.A. Fowler, G.R. Caughlan, B.A. Zimmermann, Annu. Rev. Astron. Astrophys. **5**, 525 (1967); (see also) W.A. Fowler, G.R. Caughlan, B.A. Zimmermann, Annu. Rev. Astron. Astrophys. **13**, 69 (1975)
18. A. von Engel, C.C. Goodyear, Proc. R. Soc. A **264**, 445 (1961)
19. A. Krauss, H.W. Becker, H.P. Trautvetter, C. Rolfs, Nucl. Phys. **465**, 150 (1987)

20. M. Fleischmann, S. Pons, J. Electroanal. Chem. **261**, 301 (1989); M. Fleischmann, S. Pons, J. Electroanal. Chem. **263**, 187 (1989)
21. P.L. Hagelstein et al., New Physical Effects in Metal Deuterides, in *Proc. ICCF-11, Marseille, France – Condensed Matter Nuclear Science* (World Scientific Publishing Co., Singapore, 2006), pp. 23–59, and references therein
22. Y. Arata, Y.C. Zhang, J. High Temp. Soc. **34**, 85 (2008)
23. A. Kitamura et al., Phys. Lett. A **373**, 3109 (2009), and references therein
24. Y.E. Kim, Naturwissenschaften **96**, 803 (2009), and references therein
25. Y.E. Kim, Bose-Einstein condensate theory of deuteron fusion in metal, in *Conf. Proc. Symp. on New Energy Technologies, the 239th American Chemical Society Meeting, San Francisco, USA* (2010) (to be published)
26. A. Coehn, Z. Electrochem. **35**, 676 (1929)
27. A. Coehn, W. Specht, Z. Phys. **83**, 1 (1930)
28. I. Isenberg, Phys. Rev. **79**, 736 (1950)
29. B. Duhm, Z. Phys. **94**, 435 (1935)
30. Q.M. Barer, *Diffusion in and through Solids* (Cambridge University Press, New York, 1941)
31. J.F. Macheche, J.-C. Rat, A. Herold, J. Chim. Phys. Phys. Chim. Biol. **73**, 983 (1976)
32. F.A. Lewis, Platinum Met. Rev. **26**, 20 (1982)
33. Y. Fukai, *The Metal-Hydrogen System*, 2nd edn. (Springer, Berlin, Heidelberg, New York, 2005)
34. Y.E. Kim, A.L. Zubarev, Phys. Rev. A **64**, 013603 (2001)
35. Y.E. Kim, A.L. Zubarev, Phys. Rev. A **66**, 053602 (2002)
36. Y.E. Kim, A.L. Zubarev, Italian Phys. Soc. Proc. **70**, 375 (2000)
37. Y.E. Kim. Y.J. Kim, A.L. Zubarev, J.H. Yoon, Phys. Rev. C **55**, 801 (1997)
38. Y.E. Kim, A.L. Zubarev, Fus. Technol. **37**, 151 (2000)
39. P.A.M. Dirac, *The Principles of Quantum Mechanics*, 2nd edn. (Clarendon Press, Oxford, 1935), Chap. XI, Sect. 63, p. 235
40. N. Bogoliubov, J. Phys. **11**, 23 (1966)
41. D.R. Tilley, H.R. Weller, G.M. Hale, Nucl. Phys. A **541**, 1 (1992)
42. J.M. Blatt, V.F. Weisskopf, *Theoretical Nuclear Physics* (John Wiley & Sons, Inc., 1952), 8th Printing (1972)
43. C. Rolfs, A.E. Litherland, *Nuclear Spectroscopy and Reactions, Part C*, edited by J. Cerny (Academic Press, New York, 1974), p. 143
44. R.G. Thomas, Phys. Rev. **81**, 148 (1951); R.G. Thomas, Phys. Rev. **88**, 1109 (1952)
45. C. Rolfs, H. Winkler, Phys. Lett. B **52**, 317 (1974)
46. C. Rolfs, W.S. Rodney, M.H. Shapiro, H. Winkler, Nucl. Phys. A **241**, 460 (1975)
47. C.E. Rolfs, W.S. Rodney, *Cauldrons in the Cosmos: Nuclear Astrophysics* (University of Chicago Press, 1988), Chap. 4
48. Y.E. Kim, A.L. Zubarev, Mod. Phys. Lett. B **7**, 1627 (1993); Y.E. Kim, A.L. Zubarev, Fus. Technol. **25**, 475 (1994)
49. *Handbook of Mathematical Functions with Formulas, Graphs, and Mathematical Tables*, edited by M. Abramowitz, I.A. Stegren (National Bureau of Standards Applied Mathematics Series, 1966), p. 55
50. J.R. Oppenheimer, J.S. Schwinger, Phys. Rev. **56**, 1066 (1939)
51. G.S. Chulick, Y.E. Kim, R.A. Rice, M. Rabinowitz, Nucl. Phys. A **551**, 255 (1993)
52. Y.E. Kim, Fus. Technol. **19**, 558 (1990); Y.E. Kim, AIP Conf. Proc. **228**, 807 (1990)
53. H.H. Anderson, J.F. Ziegler, *Hydrogen Stopping Powers and Ranges in All Elements* (Pergamon Press, New York, 1977)